HEFAT2012
9th International Conference on Heat Transfer, Fluid Mechanics and Thermodynamics
16 – 18 July 2012
Malta

A NUMERICAL ANALYSIS OF THE GRAETZ PROBLEM USING THE METHOD OF MOMENTS

Gu X-J. and Emerson D.R. *
*Author for correspondence
Computational Science and Engineering Department,
STFC Daresbury Laboratory,
Warrington, WA4 4AD,
England,
E-mail: david.emerson@stfc.ac.uk

ABSTRACT

In this paper, we investigate the classic Graetz problem which is concerned with the thermal development length of a fluid flowing in a pipe or channel. In our particular study, we are interested in the thermal development length associated with a rarefied gas in a 2D channel. When the gas is in a rarefied state, the boundary conditions have to be modified to account for velocity-slip and temperature-jump. Although a number of previous studies have considered rarefaction effects, they have usually taken the form of modifying the boundary conditions of the Navier-Stokes equations. Our study has involved using the Method of Moments, which represents a higher-order set of equations involving transport of stress and heat flux. The results show that the moment method captures the non-equilibrium flow features and is in good agreement with kinetic data.

INTRODUCTION

Over the past two decades, there has been an on-going acceleration of technological developments associated with micro- and nano-technology. In particular, the emergence of MEMS (Micro-Electro-Mechanical Systems), where the characteristic length scale ranges from 0.1 μm (10^{-7} m) through to millimetres, has enabled many novel ideas and concepts to be explored. It is widely accepted that major beneficiaries will be in the fields of medicine, in point-of-care medical diagnostics, biology, with the reduction and removal of animal testing, chemistry, through improving chemical yields and safe manipulation of volatile or exothermic reactions, and advanced sensors, with greatly improved sensitivity. However, there remains a general lack of progress in modelling and simulation of micro- and nano-systems. As the length scales diminish, properties often ignored at the macro-scale become critically important. For example, surface tension becomes a powerful force easily capable of blocking a fluid in a channel. In addition, boundaries can be readily modified to be either hydrophobic or hydrophilic. A crucially important factor for gaseous transport is the small characteristic length scale implies that rarefaction effects have to be taken into consideration.

Rarefied flow is characterised by the Knudsen number, Kn, which is determined from the ratio of the molecular mean free path over the width of some characteristic dimension, such as the diameter of a pipe or height of a channel. If the Knudsen number is very small (Kn<0.001), continuum theory is considered to be valid. However, over the last two decades, fabrication of micro- and nano-technology systems has made significant progress and today, many micro-electro-mechanical systems operate where the Knudsen number is above 0.001. In general, flows tend to be in the slip regime ($0.001 \le Kn < 0.1$) or transition regime ($0.1 \le Kn < 10$). Under these conditions, rarefaction effects need to be accounted for in the analysis and design of these devices. Any flow where $Kn \ge 10$ is described as a free-molecular flow and the stochastic/particle nature of the gas must be modelled through the Boltzmann equation or an equivalent approach, such as direct simulation Monte Carlo.

The thermal development characteristics of a gas flowing, or entering, a pipe or channel with a different temperature, was first analysed by Graetz [1, 2]. In his study, which described the development of a laminar flow without heat conduction and viscous dissipation, the Knudsen number was small (< 0.001) and the governing fluid dynamic equations provide an accurate description of the flow. However, with the introduction of MEMS, it is essential that the Navier-Stokes-Fourier (NSF) equations take into account velocity-slip and temperature-jump. These boundary conditions were introduced into the Graetz problem by Sparrow and Lin and other researchers [3-4] for the slip-flow regime. For flows beyond the slip-flow regime, which can be encountered in MEMS devices operating under SATP conditions when the characteristic length scale is $\le 1.0\,\mu$m, the NSF equations are no longer a reliable method of predicting flow behaviour. Many rarefied or non-equilibrium phenomena

are not embedded in the NSF equations, such as the effect of the tangential heat flux on the velocity profile. Kinetic approaches are required to describe the hydrodynamics and thermal characteristics of the flow in the transition regime. However, the solution of the Boltzmann equation or the direct simulation Monte Carlo method is computationally expensive for practical engineering applications. The Method of Moments has been developing rapidly as an alternative approach to simulating rarefied gas flows [5-7]. It bridges continuum and kinetic theory and can be used as a practical tool for engineering analysis. In the moment method, in addition to the conservation laws for mass, momentum and energy, governing equations for the heat fluxes and stresses are derived from the Boltzmann equation. More non-equilibrium phenomena are embedded in the moment equations than in the NSF equations. In this paper, the moment method is used to study convective heat transfer in a micro-channel. The gas is in the slip and early transition regime and experiences a sudden change in the wall temperature. The computed flow field and temperature distribution around the thermal change are examined. In the early transition regime, the tangential heat flux alters the velocity field in the thermally developing area and the characteristics of the heat transfer, quantified by the Nusselt number, will be discussed.

Nomenclature

$a_A^{(n)}$		coefficients for Hermite polynomials in Eq. (8)
c_i	[m/s]	intrinsic or peculiar velocity
c^2	[(m/s)^2]	$c_k c_k$
C_1, C_2		collision term constants in Eq. (19)
D_h	[m]	hydraulic diameter
f		molecular distribution function
f_M		Maxwellian distribution function
f_M^w		Maxwellian distribution function at T_w
i,j,k		tensor index
$H_A^{(n)}$		Hermite polynomials in Eq.(8)
h	[W/(m^{2}K)]	heat
Kn		Knudsen number (=λ/H)
m_{ijk}	[W/m^2]	defined in Eq.(10)
n_i		normal vector
Nu		Nusselt number
Nu^S		thermally fully developed Nusselt number
p	[Pa]	pressure
p_γ	[Pa]	defined in Eq. (27)
p_{ij}	[Pa]	pressure tensor
q_i	[W/m^2]	heat flux
q_y	[W/m^2]	heat flux normal to wall
R	[J/kgK]	specific gas constant
R_{ij}		defined in Eq. (10)
S	[K]	Sutherland's constant
T	[K]	temperature
T_w	[K]	wall temperature
$\mathbf{x}$, x_i	[m]	Cartesian axis direction
y	[m]	Cartesian axis direction
Y_1, Y_2, Y_3		collision constants in Eq. (20)

Special characters

α		accommodation coefficient
Δ		defined in Eq. (10)
δ_{ij}	[m]	Kronecker delta
ϕ_{ijkl}		fourth moment defined in Eq. (10)
λ	[m]	molecular mean free path
μ	[Pa·s]	viscosity
ρ	[kg/m^3]	density
$\rho\varepsilon$	[J]	thermal energy
$\rho_{i_1 i_2 \ldots i_N}$		N^{th} moment defined in Eq.(3)
σ_{ij}	[Pa]	deviatoric stress tensor
τ_i		tangential vector
Ω_i		high moment defined in Eq. (10)
$\boldsymbol{\xi}$, ξ_i	[m/s]	particle velocity
ψ_{ijk}		moment deviation defined in Eq. (10)
η		normalised pressure gradient $-\partial(p/p_{in})/\partial(x/H)$

Subscripts

in	Inlet condition
ex	Exit condition
w	Wall condition
o	Reference parameter

MOMENT METHOD

In Grad's moment method, once the distribution function, f, is known, its moments with respect to the particle velocity $\boldsymbol{\xi}$ can be determined. For example, the density, ρ, and the momentum, ρu_i, can be obtained from

$$\rho = \int f \, d\boldsymbol{\xi} \qquad \text{and} \qquad \rho u_i = \int \xi_i f \, d\boldsymbol{\xi} \tag{1}$$

where u_i represent the fluid velocity. It is convenient to introduce the intrinsic or peculiar velocity as

$$c_i = \xi_i - u_i \tag{2}$$

so that the moments with respect to u_i can be conveniently calculated. A set of N moments are then used to describe the state of the gas through

$$\rho_{i_1 i_2 \ldots\ldots i_N} = \int c_{i_1} c_{i_2} \ldots\ldots c_{i_N} f \, d\boldsymbol{\xi}. \tag{3}$$

Any moment can be expressed by its trace and traceless part [8]. For example, the pressure tensor can be separated as follows:

$$p_{ij} = \int c_i c_j f \, d\boldsymbol{\xi} = p\delta_{ij} + p_{<ij>} = p\delta_{ij} + \sigma_{ij}, \tag{4}$$

where δ_{ij} is the Kronecker delta function, $p = p_{kk}/3$ is the pressure, and $\sigma_{ij} = p_{<ij>}$ is the deviatoric stress tensor. The angular brackets are used to denote the traceless part of a symmetric tensor. Furthermore, the thermal energy density, ε, is given by

$$\rho\varepsilon = \frac{1}{2}\int c^2 \, f \, d\boldsymbol{\xi} = \frac{3}{2}\rho RT. \tag{5}$$

The temperature, T, is related to the pressure and density by the ideal gas law,

$$p = \rho RT, \tag{6}$$

where R is the gas constant. The heat flux vector is

$$q_i = \frac{1}{2}\int c^2 \, c_i \, f \, d\boldsymbol{\xi}. \tag{7}$$

The molecular distribution function, f, can be reconstructed from the values of its moments. Grad [9] expressed f in Hermite polynomials as:

$$f = f_M \lim_{N\to\infty} \sum_{n=0}^{N} \frac{1}{n!} a_A^{(n)} H_A^{(n)}, \tag{8}$$

where $H_A^{(n)}$ is the Hermite polynomials and $a_A^{(n)}$ are the coefficients. The Maxwellian distribution function, f_M, is expressed as

$$f_M = \frac{\rho}{\sqrt{(2\pi RT)^3}} \exp\left(-\frac{c^2}{2RT}\right). \tag{9}$$

To accurately describe the state of a gas an infinite number of moments ($N \to \infty$) is required to reconstruct the distribution function. However, for gases not too far from equilibrium, a finite number of moments should provide an adequate approximation. All the moments expressed in the truncated distribution function are regarded as the slow moment manifold [7]. The rest of the higher moments are determined by the values of the moments in the slow manifold. The truncated distribution function is often denoted as Grad's distribution function, f_G.

For the convenience of modeling, the high moments are often decomposed into the values approximated with Grad's distribution function, $\rho_{i_1 i_2 \ldots\ldots i_N}\big|_{f_G}$, and the deviation from their true value. With Grad's 26 moment distribution function, f_{G26}, the following high moments used in the present study can be expressed by

$$\begin{cases} \rho_{<ijk>} = m_{ijk} + \rho_{<ijk>|f_{G26}} = \rho_{<ijk>}, \\ \rho_{<ij>rr} = R_{ij} + \rho_{<ij>rr|f_{G26}} = R_{ij} + 7RT\sigma_{ij}, \\ \rho_{rrss} = \Delta + \rho_{rrss|f_{G26}} = \Delta + 15pRT, \\ \rho_{<ijkl>} = \phi_{ijkl} + \rho_{<ijkl>|f_{G26}} = \rho_{<ijkl>}, \\ \rho_{rr<ijk>} = \psi_{ijk} + \rho_{rr<ijk>|f_{G26}} = \psi_{ijk} + 9RTm_{ijk}, \\ \rho_{rrssi} = \Omega_i + \rho_{rrssi|f_{G26}} = \Omega_i + 28RTq_i. \end{cases} \tag{10}$$

where m_{ijk}, R_{ij}, Δ, ψ_{ijk}, ϕ_{ijkl} and Ω_i represent the difference between the true value of the higher moments and their corresponding approximation with f_{G26}. In Grad's original method, such deviations were omitted, so that m_{ijk}=R_{ij}=Δ=ψ_{ijk}= ϕ_{ijkl}=Ω_i =0.

Regularised 26 Moment Equations

Combining Grad's moment method [9] and regularisation procedure [5], a system of 26 moment equations for monatomic gas flow are developed by [7]

$$\frac{\partial \rho}{\partial t} + \frac{\partial \rho u_i}{\partial x_i} = 0, \tag{11}$$

$$\frac{\partial \rho u_i}{\partial t} + \frac{\partial \rho u_i u_j}{\partial x_j} + \frac{\partial \sigma_{ij}}{\partial x_j} = -\frac{\partial p}{\partial x_i}, \tag{12}$$

$$\frac{\partial \rho T}{\partial t} + \frac{\partial \rho u_i T}{\partial x_i} + \frac{2}{3R}\frac{\partial q_i}{\partial x_i} = -\frac{2}{3R}\left(p\frac{\partial u_i}{\partial x_i} + \sigma_{ij}\frac{\partial u_j}{\partial x_i}\right), \tag{13}$$

$$\begin{aligned} &\frac{\partial \sigma_{ij}}{\partial t} + \frac{\partial u_k \sigma_{ij}}{\partial x_k} + \frac{\partial m_{ijk}}{\partial x_k} = -\frac{p}{\mu}\sigma_{ij} - 2p\frac{\partial u_{<i}}{\partial x_{j>}} - \frac{4}{5}\frac{\partial q_{<i}}{\partial x_{j>}} \\ &-2\sigma_{k<i}\frac{\partial u_{j>}}{\partial x_k}, \end{aligned} \tag{14}$$

$$\begin{aligned} &\frac{\partial q_i}{\partial t} + \frac{\partial u_j q_i}{\partial x_j} + \frac{1}{2}\frac{\partial R_{ij}}{\partial x_j} = -\frac{2}{3}\frac{p}{\mu}q_i - \frac{5}{2}pR\frac{\partial T}{\partial x_i} \\ &-\frac{7\sigma_{ik}R}{2}\frac{\partial T}{\partial x_k} - \frac{2}{5}\left(\frac{7}{2}q_k\frac{\partial u_i}{\partial x_k} + q_k\frac{\partial u_k}{\partial x_i} + q_i\frac{\partial u_k}{\partial x_k}\right) \\ &-RT\frac{\partial \sigma_{ik}}{\partial x_k} + \frac{\sigma_{ij}}{\rho}\left(\frac{\partial p}{\partial x_j} + \frac{\partial \sigma_{jk}}{\partial x_k}\right) - \frac{1}{6}\frac{\partial \Delta}{\partial x_i} - m_{ijk}\frac{\partial u_j}{\partial x_k}, \end{aligned} \tag{15}$$

$$\begin{aligned} &\frac{\partial m_{ijk}}{\partial t} + \frac{\partial u_l m_{ijk}}{\partial x_l} + \frac{\partial \phi_{ijkl}}{\partial x_l} = -\frac{3}{2}\frac{p}{\mu}m_{ijk} - 3p\frac{\partial\left(\sigma_{<ij}/\rho\right)}{\partial x_{k>}} \\ &+3\frac{\sigma_{<ij}}{\rho}\frac{\partial \sigma_{k>l}}{\partial x_l} - \frac{12}{5}q_{<i}\frac{\partial u_j}{\partial x_{k>}} - 3m_{l<ij}\frac{\partial u_{k>}}{\partial x_l} - \frac{3}{7}\frac{\partial R_{<ij}}{\partial x_{k>}}, \end{aligned} \tag{16}$$

$$\begin{aligned} &\frac{\partial R_{ij}}{\partial t} + \frac{\partial u_k R_{ij}}{\partial x_k} + \frac{\partial \psi_{ijk}}{\partial x_k} = -\frac{7}{6}\frac{p}{\mu}R_{ij} - \frac{28}{5}p\frac{\partial\left(q_{<i}/\rho\right)}{\partial x_{j>}} \\ &-\frac{2}{3}\frac{p}{\mu}\frac{\sigma_{k<i}\sigma_{j>k}}{\rho} - \frac{28}{5}q_{<i}\frac{\partial RT}{\partial x_{j>}} + \frac{28}{5}\frac{q_{<i}}{\rho}\frac{\partial \sigma_{j>k}}{\partial x_k} \\ &-2RT\frac{\partial m_{ijk}}{\partial x_k} - 9m_{ijk}\frac{\partial RT}{\partial x_k} + \frac{14}{3}\frac{\sigma_{ij}}{\rho}\left(\frac{\partial q_k}{\partial x_k} + \sigma_{kl}\frac{\partial u_k}{\partial x_l}\right) \\ &-2\phi_{ijkl}\frac{\partial u_k}{\partial x_l} - 4RT\left(\sigma_{k<i}\frac{\partial u_k}{\partial x_{j>}} + \sigma_{k<i}\frac{\partial u_{j>}}{\partial x_k} - \frac{2}{3}\sigma_{ij}\frac{\partial u_k}{\partial x_k}\right) \\ &+2\frac{m_{ijk}}{\rho}\left(\frac{\partial p}{\partial x_k} + \frac{\partial \sigma_{kl}}{\partial x_l}\right) - \frac{14}{15}\Delta\frac{\partial u_{<i}}{\partial x_{j>}} - \frac{2}{5}\frac{\partial \Omega_{<i}}{\partial x_{j>}} \\ &-\left(\frac{6}{7}R_{<ij}\frac{\partial u_{k>}}{\partial x_k} + \frac{4}{5}R_{k<i}\frac{\partial u_k}{\partial x_{j>}} + 2R_{k<i}\frac{\partial u_{j>}}{\partial x_k}\right) \end{aligned} \tag{17}$$

and

$$\begin{aligned} &\frac{\partial \Delta}{\partial t} + \frac{\partial \Delta u_i}{\partial x_i} + \frac{\partial \Omega_i}{\partial x_i} = -\frac{2}{3}\frac{p}{\mu}\Delta - 8p\frac{\partial\left(q_i/\rho\right)}{\partial x_i} \\ &-\frac{2}{3}\frac{p}{\mu}\frac{\sigma_{ij}\sigma_{ij}}{\rho} - 4\left(2RT\sigma_{ij} + R_{ij}\right)\frac{\partial u_i}{\partial x_j} + 8\frac{q_i}{\rho}\frac{\partial \sigma_{ij}}{\partial x_j} \\ &-20q_i\frac{\partial RT}{\partial x_i} - \frac{4}{3}\Delta\frac{\partial u_i}{\partial x_i}, \end{aligned} \tag{18}$$

where t and x_i are temporal and spatial coordinates, respectively, and μ is the viscosity. Any suffix i, j, k represents the usual summation convention. In addition to the conservation laws (11)-(13) and the governing equations (14) and (15) for the deviatoric stress, σ_{ij}, and heat flux, q_i, the governing equations (16)-(18) for the higher moments m_{ijk}, R_{ij} and Δ are included in the 26 moment system. The above equation set is closed by the following constitutive relationships [7]:

$$\phi_{ijkl} = -\frac{4\mu}{C_1}\frac{\partial\left(m_{<ijk}/\rho\right)}{\partial x_{l>}} + \frac{4\mu}{C_1 p\rho} m_{<ijk}\frac{\partial \sigma_{l>m}}{\partial x_m}$$
$$-\frac{12}{C_1}\frac{\mu}{\rho}\sigma_{<ij}\frac{\partial u_k}{\partial x_{l>}} - \frac{12}{7}\frac{\mu R_{<ij}}{C_1 p}\frac{\partial u_k}{\partial x_{l>}} - \frac{C_2}{C_1}\frac{\sigma_{<ij}\sigma_{kl>}}{\rho}, \quad (19)$$

$$\psi_{ijk} = -\frac{27\mu}{7Y_1}\frac{\partial\left(R_{<ij}/\rho\right)}{\partial x_{k>}}$$
$$-\frac{27}{7}\frac{\mu}{Y_1 p}\left(R_{<ij} + 7RT\sigma_{<ij}\right)\frac{\partial RT}{\partial x_{k>}}$$
$$-\frac{108}{5Y_1}\frac{\mu}{\rho}q_{<i}\frac{\partial u_j}{\partial x_{k>}} + \frac{6\mu}{Y_1 p}\frac{m_{ijk}}{\rho}\left(\frac{\partial q_m}{\partial x_m} + \sigma_{ml}\frac{\partial u_m}{\partial x_l}\right) \quad (20)$$
$$-\frac{\mu}{Y_1\rho}\left(\frac{54}{7}m_{m<ij}\frac{\partial u_m}{\partial x_{k>}} + 8m_{<ijk}\frac{\partial u_{m>}}{\partial x_m} - 6m_{ijk}\frac{\partial u_m}{\partial x_m}\right)$$
$$+\frac{27\mu}{7Y_1}\frac{R_{<ij}}{p\rho}\frac{\partial \sigma_{k>m}}{\partial x_m} - \left(\frac{Y_2}{Y_1}\frac{\sigma_{<li}m_{jkl>}}{\rho} + \frac{Y_3}{Y_1}\frac{q_{<i}\sigma_{jk>}}{\rho}\right)$$

$$\psi_{ijk} = -\frac{27\mu}{7Y_1}\frac{\partial\left(R_{<ij}/\rho\right)}{\partial x_{k>}}$$
$$-\frac{27}{7}\frac{\mu}{Y_1 p}\left(R_{<ij} + 7RT\sigma_{<ij}\right)\frac{\partial RT}{\partial x_{k>}}$$
$$-\frac{108}{5Y_1}\frac{\mu}{\rho}q_{<i}\frac{\partial u_j}{\partial x_{k>}} + \frac{6\mu}{Y_1 p}\frac{m_{ijk}}{\rho}\left(\frac{\partial q_m}{\partial x_m} + \sigma_{ml}\frac{\partial u_m}{\partial x_l}\right) \quad (21)$$
$$-\frac{\mu}{Y_1\rho}\left(\frac{54}{7}m_{m<ij}\frac{\partial u_m}{\partial x_{k>}} + 8m_{<ijk}\frac{\partial u_{m>}}{\partial x_m} - 6m_{ijk}\frac{\partial u_m}{\partial x_m}\right)$$
$$+\frac{27\mu}{7Y_1}\frac{R_{<ij}}{p\rho}\frac{\partial \sigma_{k>m}}{\partial x_m} - \left(\frac{Y_2}{Y_1}\frac{\sigma_{<li}m_{jkl>}}{\rho} + \frac{Y_3}{Y_1}\frac{q_{<i}\sigma_{jk>}}{\rho}\right)$$

and

$$\Omega_i = -\frac{7\mu}{3}\frac{\partial\left(\Delta/\rho\right)}{\partial x_i} - 4\mu\frac{\partial\left(R_{ij}/\rho\right)}{\partial x_j} - 8\frac{\mu}{\rho}m_{ijk}\frac{\partial u_j}{\partial x_k}$$
$$-\frac{56}{5}\frac{\mu}{\rho}q_j\left(\frac{\partial u_i}{\partial x_j} + \frac{\partial u_j}{\partial x_i}\right) - 14\frac{\mu}{p}\left(2RT\sigma_{ij} + R_{ij}\right)\frac{\partial RT}{\partial x_j} \quad (22)$$
$$+\frac{56}{3}\frac{\mu}{p}\frac{q_i}{\rho}\left(\frac{\partial q_j}{\partial x_j} + \sigma_{jk}\frac{\partial u_j}{\partial x_k}\right) + 4\frac{\mu}{p}\frac{R_{ij}}{\rho}\frac{\partial \sigma_{jk}}{\partial x_k}$$
$$+\frac{7}{3}\frac{\mu}{p}\Delta\left(\frac{\partial \sigma_{ij}}{\rho\partial x_j} - 2\frac{\partial RT}{\partial x_i}\right) - \frac{2}{15}\left(\frac{5m_{ijk}\sigma_{jk} + 14q_j\sigma_{ij}}{\rho}\right),$$

in which, C_1=2.097, C_2=-0.291, Y_1=1.82, Y_2=-1.203 and Y_3=0.854 are collision term constants [7].

The regularisation of Grad's moment equations allows the higher moments to approach the slow moment manifold with a fast but finite rate, a procedure which enhances the capability of the moment method significantly.

Numerical Algorithm

In the moment system, the higher moment provides the transport mechanism for the moment one order lower [7]. For a gas flow close to the equilibrium state, a sufficient number of molecular isotropic collisions cause the flow to behave as a continuum and the gradient transport mechanism prevails. As the value of *Kn* increases, a non-gradient transport mechanism occurs in addition to the conventional gradient transport mechanism familiar in continuum methods. In fact, both gradient and non-gradient mechanisms co-exist in the transition regime. This feature has been used to construct the numerical algorithm for low speed flow in confined geometries [6,7].

The regularised moment equations are a mixed set of first and second order partial differential equations. Traditionally, these equations are used to study hyperbolic flows [10]. In the case of low speed gas flow, the flow is parabolic or elliptic. Using a hyperbolic flow solver to solve elliptic flows is inefficient and expensive. To overcome this issue, the moments are decomposed into their gradient (hydrodynamic) and non-gradient (non-hydrodynamic) transport parts. As a result, the moment equations can be recast in convection-diffusion form. These equations form a set of second order partial differential equations and the mathematical characteristics of the system will be determined by the flow conditions. They are of a hyperbolic nature for high speed flows and parabolic or elliptic when the flow velocity is low or the flow is re-circulating. In this way, traditional CFD techniques for low speed flows can be used. In the present study, the finite volume approach has been employed. The diffusion and source terms are discretised by a central difference scheme. For the convective terms, a range of upwind schemes are available. The SIMPLE algorithm is adopted to resolve the coupling of the velocity and pressure fields. A collocated grid arrangement is used and any non-physical pressure oscillations are eliminated by the interpolation scheme of Rhie and Chow.

Wall boundary conditions

To apply the moment equations to flows in confined geometries, appropriate wall boundary conditions are required to determine a unique solution. One of the difficulties encountered in any investigation of wall boundary conditions is due to a limited understanding of the structure of surface layers of solid bodies and of the effective interaction potential of the gas molecules with the wall. A scattering kernel represents a fundamental concept in gas-surface interactions, by means of which other quantities should be defined [11].

Maxwell's kinetic boundary condition [12] is one of the simplest models and it states that a fraction, (1-α), of gas molecules will undergo specular reflection while the remaining fraction, α, will be diffusely reflected with a Maxwellian distribution, f_M^w, at the temperature of the wall, T_w. In a frame where the coordinates are attached to the wall, with n_i the normal vector of the wall pointing towards the gas and τ_i the tangential vector of the wall, such that all molecules with $\xi_i n_i$<0 are incident upon the wall and molecules with $\xi_i n_i \geq 0$ are emitted by the wall, Maxwell's boundary condition can be expressed by [8]:

$$f^w = \begin{cases} \alpha f_M^w + (1-\alpha) f(-\xi_i n_i), & \xi_i n_i \geq 0, \\ f(\xi_i n_i), & \xi_i n_i < 0. \end{cases} \quad (23)$$

By definition, the value of any moment at the wall can be obtained from

$$\int c_{i_1} c_{i_2} \cdots c_{i_n} f d\boldsymbol{\xi} = \int c_{i_1} c_{i_2} \cdots c_{i_n} f^w d\boldsymbol{\xi} \tag{24}$$

However, Grad [9] considered the special case of $\alpha = 0$ and concluded that only those moments that are odd functions of $\xi_i n_i$ can be used to construct the wall boundary conditions. The details of the construction procedure of the macroscopic wall boundary conditions for the moment equations are given in Ref. [6, 7]. The slip velocity parallel to the wall, u_τ, and the temperature jump condition can be expressed as

$$u_\tau = -\frac{2-\alpha}{\alpha}\sqrt{\frac{\pi RT}{2}}\frac{\sigma_{n\tau}}{p_\gamma} \underline{-\frac{5m_{nn\tau}+2q_\tau}{10p_\gamma}+\frac{9\Omega_\tau+70\psi_{nn\tau}}{2520p_\gamma RT}} \tag{25}$$

and

$$RT - RT_w = -\frac{2-\alpha}{\alpha}\sqrt{\frac{\pi RT}{2}}\frac{q_n}{2p_\gamma} \underline{-\frac{RT\sigma_{nn}}{4p_\gamma}+\frac{u_\tau^2}{4}-\frac{75R_{nn}+28\Delta}{840p_\gamma}+\frac{\phi_{nnnn}}{24p_\gamma}} \tag{26}$$

Where

$$p_\gamma = p + \frac{\sigma_{nn}}{2} - \frac{30R_{nn}+7\Delta}{840RT} - \frac{\phi_{nnnn}}{24RT}. \tag{27}$$

Here $\sigma_{nn}=\sigma_{ij}n_in_j$, $\sigma_{n\tau}=\sigma_{ij}n_i\tau_j$, $m_{nn\tau}=m_{ijk}n_in_j\tau_k$, $m_{nnn}=m_{ijk}n_in_jn_k$, $q_\tau=q_i\tau_i$, $R_{nn}=R_{ij}n_in_j$, $\Omega_\tau=\Omega_i\tau_i$, $\psi_{\mathrm{nn\tau}}=\psi_{ijk}n_in_j\tau_k$, and $\phi_{nnnn}=\phi_{ijkl}n_in_jn_kn_l$ are the tangential and normal components of σ_{ij}, q_i, m_{ijk}, R_{ij}, ψ_{ijk}, ϕ_{ijkl} and Ω_i relative to the wall, respectively. It should be noted that the normal velocity at the wall, $u_n = 0$, since there is no gas flow through the wall. Equations (25) and (26) are similar to the slip velocity and temperature jump conditions for the NSF equations [13, 14] with the underlined terms on the right hand side providing higher-order moment corrections. These underlined terms can be related to second- or higher-order velocity-slip and temperature-jump boundary conditions [15]. With a normalized slip velocity, $\hat{u}_\tau = u_\tau/\sqrt{RT}$, and a normalised wall temperature, $\hat{T}_w = T_w/T$, the rest of the wall boundary conditions are:

$$\sigma_{\tau\tau} = -\frac{2-\alpha}{\alpha}\sqrt{\frac{\pi RT}{2}}\left(\frac{5m_{n\tau\tau}+2q_n}{5RT}\right) + p_\gamma\left(\hat{u}_\tau^2+\hat{T}_w-1\right) - \frac{R_{\tau\tau}+R_{nn}}{14RT} - \frac{\Delta}{30RT} - \frac{\phi_{nn\tau\tau}}{2RT}, \tag{28}$$

$$\sigma_{nn} = -\frac{2-\alpha}{\alpha}\sqrt{\frac{\pi RT}{2}}\left(\frac{5m_{nnn}+6q_n}{10RT}\right) + p_\gamma\left(\hat{T}_w-1\right) - \frac{R_{nn}}{7RT} - \frac{\Delta}{30RT} - \frac{\phi_{nnnn}}{6RT}, \tag{29}$$

$$q_\tau = -\frac{5}{18}\frac{2-\alpha}{\alpha}\sqrt{\frac{\pi RT}{2}}\left(7\sigma_{n\tau}+\frac{R_{n\tau}}{RT}\right) - \frac{10m_{nn\tau}}{9} - \frac{5\psi_{nn\tau}}{81RT} - \frac{\Omega_\tau}{56RT} - \frac{5\hat{u}_\tau p_\gamma\sqrt{RT}\left(\hat{u}_\tau^2+6\hat{T}_w\right)}{18}, \tag{30}$$

$$m_{\tau\tau\tau} = -\frac{2-\alpha}{\alpha}\sqrt{\frac{\pi RT}{2}}\left(3\sigma_{n\tau}+\frac{3R_{n\tau}}{7RT}+\frac{\phi_{n\tau\tau\tau}}{RT}\right) - \frac{3m_{nn\tau}}{2} - \frac{9q_\tau}{5} - p_\gamma\hat{u}_\tau\sqrt{RT}\left(\hat{u}_\tau^2+3\hat{T}_w\right) - \frac{9\Omega_\tau}{280RT} - \frac{2\psi_{\tau\tau\tau}+3\psi_{nn\tau}}{36RT}, \tag{31}$$

$$m_{nn\tau} = -\frac{2-\alpha}{\alpha}\sqrt{\frac{\pi RT}{2}}\left(\sigma_{\tau n}+\frac{R_{n\tau}}{7RT}+\frac{\phi_{nnn\tau}}{3RT}\right) - \frac{2}{5}q_\tau - \frac{2\hat{T}_w\hat{u}_\tau p_\gamma\sqrt{RT}}{3} - \frac{\psi_{nn\tau}}{18RT} - \frac{\Omega_\tau}{140RT}, \tag{32}$$

$$R_{\tau\tau} = -\frac{2-\alpha}{\alpha}\sqrt{\frac{\pi RT}{2}}\left(\frac{28q_n}{15}+\frac{14m_{n\tau\tau}}{3}\right) - \frac{2-\alpha}{\alpha}\sqrt{\frac{\pi RT}{2}}\left(\frac{\Omega_n}{15RT}+\frac{14\psi_{n\tau\tau}}{27RT}\right) + \frac{7p_\gamma RT\left(\hat{u}_\tau^4+6\hat{T}_w\hat{u}_\tau^2+3\hat{T}_w^2-3\right)}{9} - \frac{14RT\sigma_{\tau\tau}}{3} - \frac{R_{nn}}{3} - \frac{14\Delta}{45} - \frac{7\left(\phi_{\tau\tau\tau\tau}+3\phi_{nn\tau\tau}\right)}{9}, \tag{33}$$

$$R_{nn} = -\frac{2-\alpha}{\alpha}\sqrt{\frac{\pi RT}{2}}\left(\frac{21q_n}{8}+\frac{35m_{nnn}}{16}\right) - \frac{2-\alpha}{\alpha}\sqrt{\frac{\pi RT}{2}}\left(\frac{35\psi_{nnn}}{144RT}+\frac{3\Omega_n}{32RT}\right) + \frac{7p_\gamma RT\left(\hat{T}_w^2-1\right)}{4} - \frac{7RT\sigma_{nn}}{2} - \frac{7\Delta}{30} - \frac{7\phi_{nnnn}}{6}, \tag{34}$$

and

$$\Delta = -\frac{35}{4}\frac{2-\alpha}{\alpha}\sqrt{\frac{\pi RT}{2}}\left(q_n+\frac{\Omega_n}{28RT}\right) - \frac{15}{4}RT\sigma_{nn} - \frac{5}{4}p_\gamma RT\left(6-6\hat{T}_w^2-\frac{\hat{u}_\tau^4}{4}-3\hat{u}_\tau^2\hat{T}_w\right) - \frac{15}{8}R_{nn} + \frac{35}{48}\phi_{nnnn}. \tag{35}$$

RESULTS AND DISCUSSIONS

In the present study, the flow of a gas through a two-dimensional channel with a width of H is considered. Pressure at the channel entrance p_{in} and exit p_{ex} is assumed uniform with a small pressure gradient $\eta = -\partial(p/p_{in})/\partial(x/H)$. A gas with a temperature T_o enters the channel with a wall temperature at T_w. The Knudsen number is given by $Kn=\lambda/H$, where the mean free path, λ, is defined by [11,13]

$$\lambda = \frac{\mu_o}{p_{in}}\sqrt{\frac{\pi R T_o}{2}} \qquad (36)$$

The viscosity was obtained from Sutherland's law [16]:

$$\mu = \mu_o \left(\frac{T}{T_o}\right)^{1.5} \frac{T_o + S}{T + S}, \qquad (37)$$

where the reference viscosity and temperature are given by μ_o=21.25×10^{-6} Pa·s and T_o=273 K, respectively. The specific gas constant and Sutherland's constant for argon are R=208J/kg·K and S=144 K. The accommodation coefficient, α, is assigned a value of unity i.e. fully diffuse reflection has been assumed for all the walls. The wall temperature T_w is 5 K above the initial gas temperature.

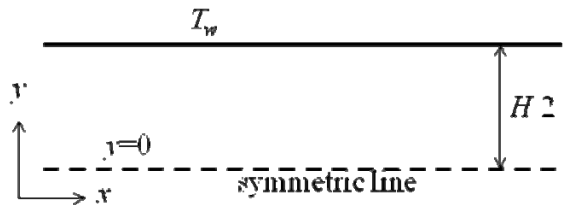

Figure 1 Channel geometry

The NSF equations and the R26 equations are solved for the flow with 150×50 equi-spaced grid points across a domain with 25μm×5μm and the symmetry condition is employed at y = 0 μm as shown in **Figure 1.** In the present study, the Brinkman number is set to equal to zero, i.e. the viscous dissipation terms in the energy equation (13) are switched off, to be consistent with theoretical analysis [1-4, 17]. Shown in **Figure 2** are the velocity vectors imposed on the temperature field from the R26 equation for the case Kn=0.1. The thermal field develops much slower than the hydrodynamic field.

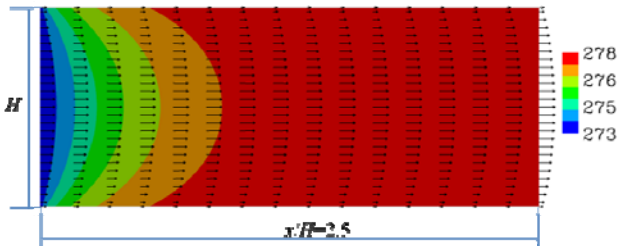

Figure 2 The computed velocity vectors and temperature field from the R26 equations for Kn=0.1, T_w=278 K and T_o=273 K.

The normalised velocity u/u_o at x/H=1 predicted by both the NSF with the second order slip boundary condition and the R26 equations is presented in **Figure 3**, where $u_o = \eta\sqrt{2RT_o}$. The NSF equations with second-order slip boundary condition predict a larger slip velocity than the R26 equation [7].

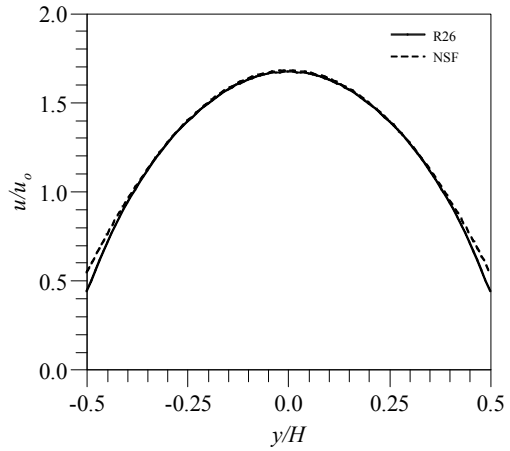

Figure 3 The predicted velocity profile at x/H=1 for Kn=0.1.

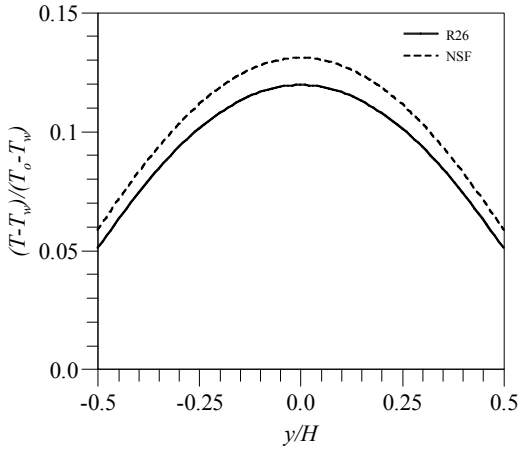

Figure 4 The predicted temperature profile at x/H=1 for Kn=0.1.

The computed temperature profile at x/H=1 is shown in **Figure 4** for Kn=0.1. Again the NSF equations predict a higher temperature jump than the R26 equations.

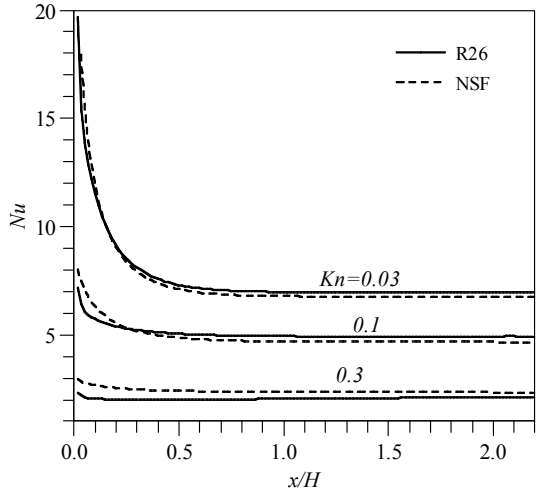

Figure 5 The predicted development of the Nusselt number for different values of Kn.

The heat transfer between the gas and the walls can be meaured by the heat transfer coeffcient, h, which is defined as,

$$h\left(T_b - T_w\right) = q_y \,. \tag{38}$$

Here, T_b is the bulk temperature defined by

$$T_b = \frac{\int_{-H/2}^{H/2} \rho u T dy}{\int_{-H/2}^{H/2} \rho u dy} \,. \tag{39}$$

The Nusselt number, the non-dimensional heat transfer coefficient, is defined by

$$Nu = \frac{D_h h}{\kappa} = \frac{2Hh}{\kappa}, \tag{40}$$

and has been studied in the slip regime analytically for channel flows [1-4,17], where D_h=2H is the hydraulic diameter of the channel. In the present study, the Nusselt number can be readily calculated from the solutions of NSF and the R26 equations. Shown in **Figure 5** is the development of Nu when a gas enters into a channel of a different temperature. When the Knudsen number is small, the value of Nu is large at the entrance. As the gas flows into the channel, the value of Nu decreases to a constant, Nu^S. As Kn increases, the development process becomes shorter. In the slip regime, the NSF equations give a lower value of Nu than the R26 equations, whilst in the early transition regime, we obtain the opposite effect. The values of the fully developed Nusselt number, Nu^S, predicted from different approaches for different Kn are shown in **Figure 6.** In the slip regime, the values of Nu^S from the continuum equations and kinetic theory are close to each. In the early transition regime, the R26 equations produce the values of Nu^S close to the results from DSMC [17]. The NSF equations overpredict the value of Nu^S as expected.

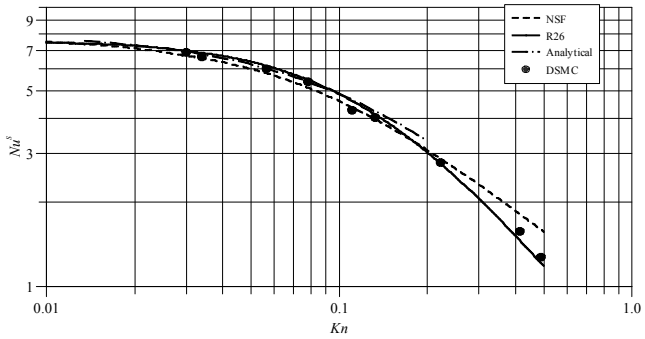

Figure 6 Fully developed Nusselt number at different values of Kn.

CONCLUSIONS

The paper has investigated the classic Graetz thermal development length problem for the case of a rarefied gas entering a micro-channel. To capture the non-equilibrium flow phenomena, the Method of Moments has been employed. Results are compared to predictions from the Navier-Stokes-Fourier equations and the regularized 26 moment equations. We show that the thermal field develops much slower than the hydrodynamic field and rarefaction effects are better captured by the moment method, particularly at higher Knudsen numbers where agreement with data from kinetic theory is very good.

ACKNOWLEDGEMENTS

The authors would like to thank the Engineering and Physical Sciences Research Council (EPSRC) for their support of CCP12 and DRE under the Programme Grant award for *Non-Equilibrium Fluid Dynamics for Micro/Nano Engineering Systems* (grant number EP/I011927/1).

REFERENCES

[1] Graetz, L., Uber die Warmeleitungsfahigheit von Flussingkeiten, part 1, *Annalen der Physik und Chemie*, vol 18, 1883, pp.79-94.

[2] Graetz, L., Uber die Warmeleitungsfahigheit von Flussingkeiten, part 2, *Annalen der Physik und Chemie*, vol 25, 1885, pp. 337-357.

[3] Sparrow, E. M., and Lin, S. H., Laminar heat transfer in tubes under slip flow conditions, *J. Heat Transfer*, vol, 84, 1962, pp. 363-369.

[4] Barron, R. F., Wang, X., Ameel, T. A. and Warrington, R. O., The Graetz problem extended to slip flow, *Int. J. Heat Mass Transfer*, vol. 40, 1997, 1817-1823.

[5] Struchtrup, H. and Torrilhon, M., Regularization of Grad's 13 Moment Equations: Derivation and Linear Analysis, *Phys. Fluids*, vol. 15, 2003, pp. 2668-2680.

[6] Gu, X. J. and Emerson, D. R., A Computational Strategy for the Regularized 13 Moment Equations with Enhanced Wall-boundary Conditions, *J. Comput. Phys*., vol. 225, 2007, pp. 263-283.

[7] Gu, X. J. and Emerson, D. R., A High-order Moments Approach for Capturing Nonequilibrium Phenomena in the Transition Regime, *J. Fluid Mech*., 636, 2009, pp.177-216.

[8] Struchtrup, H., Macroscopic Transport Equations for Rarefied Gas Flows. Springer-Verlag, Berlin Heidelberg, 2005.

[9] Grad, H., On the Kinetic Theory of Rarefied Gases, Commun. *Pure Appl. Math.*, vol. 2, 1949, pp. 331-407.

[10]Torrilhon, M. and Struchtrup, H., Regularized 13 Moment Equation: Shock Structure Calculations and Comparison to Burnett Models, *J. Fluid Mech*. Vol. 513, 2004, pp. 171-198.

[11] Cercignani, C., Rarefied Gas Dynamics: From Basic Concepts to Actual Calculations, Cambridge University, 2000.

[12] Maxwell, J. C., On Stresses in Rarified Gases Arising From Inequalities of Temperature, *Phil. Trans. Roy. Soc*. (Lond.) vol. 170, 1879, pp. 231-256.

[13] Cercignani, C., 1988, The Boltzmann Equation and Its Applications, Springer, New York.

[14] Gad-el-hak, M., 1999, "The Fluid Mechanics of Microdevices - The Freeman Scholar Lecture," *J. Fluids Eng.*, 121, pp. 5-33.

[15] Struchtrup, H. and Torrilhon, M., Higher Order Effects in Rarefied Channel Flows, *Phys. Rev. E*, vol. 78, 2008, 046301.

[16] White, F. M., Viscous Fluid Flow. McGraw-Hill, Inc, New York, 1991.

[17] Hadjiconstantinou, N. G., Constant-Wall-Temperature Nusselt Number in Micro and Nano-Channels, *J. Heat Transfer*, vol. 124, 2002, pp. 356-365.